

# Predominance of thermal contact resistance in a silicon nanowire on a planar substrate

Yann Chalopin,<sup>\*</sup> Jean-Numa Gillet, and Sebastian Volz

Laboratoire d'Energétique Moléculaire et Macroscopique, Combustion CNRS UPR 288, Ecole Centrale Paris, Grande Voie des Vignes,  
F-92295 Châtenay-Malabry Cedex, France

(Received 16 April 2008; published 25 June 2008)

At low temperatures, thermal transport in single crystalline nanowires with sub-10-nm diameters is defined in terms of the universal quantum of conductance. In the case of a nanowire connected to plane substrates, additional conductances appear due to the contacts. We calculate the contact conductances and prove that they are much smaller than the conductance of the nanowire. The reason is that the number of excited modes per unit volume in the substrates becomes smaller than the one in the wire at low temperatures. The substrate then generates the predominant thermal resistance because its specific heat becomes smaller than the one of the wire. From these considerations, the wire-membrane and membrane-plane substrate thermal conductances can also be predicted.

DOI: 10.1103/PhysRevB.77.233309

PACS number(s): 63.22.-m, 63.20.D-, 65.80.+n, 66.70.-f

## I. INTRODUCTION

Over the last decade, there has been tremendous advancement in novel approaches to manage thermal transport in single crystalline nanowires since future electronics driving force is turned on size reduction.<sup>1</sup> Silicon nanowires with diameters approaching the 10 nm scale are also involved in biosensors,<sup>2</sup> thermoelectric cooling, and probing such as in mass spectrometry.<sup>3</sup> These wires are generally electrically heated and key parameters such as thermal and electrical resistances are difficult to characterize.

In these systems at low temperatures, the wave behavior of phonons is predominant over the phonon-particle effects<sup>4-6</sup> when the wavelength of the main carriers approaches the wire diameter. Accordingly, heat conduction in one-dimensional (1D) structures is usually defined as a function of the universal quantum of conductance. Previous works<sup>7,8</sup> beautifully verified the transport of this quantum at low enough temperatures through a junction. The junction shape was designed in such a way that phonon modes were fully transmitted. However, further studies<sup>9-11</sup> based on long nanowires could not highlight the same behavior and proved the dependence on  $T^3$  for the wire conductance. In long nanowires, eigenmodes are mostly defined by the wire structure rather than by the contacts with the reservoirs. The consecutive mismatch in eigenmodes between wire and reservoir implies that phonons are only partially transmitted at the contacts and additional thermal conductances arise.

We highlight that the analysis of this mismatch leads to a counterintuitive conclusion. The substrates contain an infinite number of modes because their density of states (DOS) is proportional to volume. In addition, three-dimensional infinite bodies are indeed thermal reservoirs when they are coupled to the volume of the thermalized object. However, when the coupling is through a surface and through a heat flux, then the DOS per unit volume, which is finite, is the key quantity. The number of excited modes per unit volume in the substrate is proportional to temperature to the power three, whereas the one in the wire is proportional to temperature. Consequently, the number of excited modes in the substrate becomes smaller than the one in the wire at low temperatures. The substrate then generates the predominant resistance because its specific heat becomes smaller than the

one of the wire. The point of this Brief Report is to take a very direct path to show that the contact resistance and the resistance of the total system (substrate-wire-substrate) do not depend on the nanowire but on the planar substrates contributions only.

We have computed the thermal contact conductance between the wire and the thermal reservoir. An abrupt junction as well as any larger shape of contact would lead to the same conductance within a few percent. We observe that the contact conductance is by far smaller than that of the nanowire when the temperature  $T < 30$  K, and we explain the governing physical mechanisms.

In the first part, the thermal conductance at contact is expressed as a function of heat capacities and group velocities of both nanowire and substrate. The calculation is carried out by deriving the dispersion curves and the group velocities in the nanowire. The resulting thermal conductances and the impact of the density of states mismatch are finally discussed.

## II. THERMAL CONDUCTANCE BETWEEN THE NANOWIRE AND THE PLANAR SUBSTRATE

### A. Model

The thermal conductance between the wire and the substrate is derived from the net energy flux<sup>12,13</sup> defined as a sum of two counterpropagative currents,

$$Q = t_b Q_b - t_w Q_w, \quad (1)$$

$Q_b$ ,  $Q_w$ ,  $t_b$ , and  $t_w$  correspond to the heat fluxes and transmission coefficients from the substrate to the wire and from the wire to the substrate, respectively. The contact conductance  $G$  is obtained by expressing the heat flux  $Q$  as linearly dependent on the temperature drop at the contact:  $Q = G(T_w - T_b)$ . The indexes  $w$  and  $b$  refer to the wire and substrate, respectively. The Taylor expansion of Eq. (1) yields

$$Q = t_b \left[ Q_b(\bar{T}) - \Delta T \frac{\partial Q_b}{\partial T_b} \right] - t_w \left[ Q_w(\bar{T}) + \Delta T \frac{\partial Q_w}{\partial T_w} \right], \quad (2)$$

where  $2\bar{T} = T_b + T_w$  and  $2\Delta T = T_b - T_w$ . Stating that the heat flux is zero when the temperature difference vanishes, i.e.,

$t_b Q_b(\bar{T}) = t_w Q_w(\bar{T})$ , leads to the following expression for the thermal conductance:

$$G = \frac{1}{2} \left( t_b \frac{\partial Q_b}{\partial T_b} + t_w \frac{\partial Q_w}{\partial T_w} \right) = \frac{1}{2} (t_b C_b v_b + t_w C_w v_w) \quad (3)$$

The second equality including heat capacity  $C$  and average group velocity  $v$  was proven in Ref. 14.

### B. Transmission coefficient at contact

Since we want to show the predominance of the contact resistance over the wire resistance, we choose the model that tends to overestimate transmission, i.e., the diffuse limit approximation.<sup>15,16</sup>

$$t_w = \frac{C_b v_b}{C_b v_b + C_w v_w}. \quad (4)$$

Inverting indexes  $w$  and  $b$  provides the transmission coefficient  $t_b$  from the substrate to the wire. This model implies that phonons lose their memories when they leave the interface in such a way that the transmission  $t_w$  from the wire to the reservoir can also be assimilated as the reflection coefficient of phonons coming from the reservoir.

Combining this model with Eq. (3) yields the following expression for the thermal conductance:

$$\frac{1}{G} = \frac{1}{C_w v_w} + \frac{1}{C_b v_b}. \quad (5)$$

The contact conductance appears as the combination of two conductances in series. Each conductance corresponds to a ballistic phonon flux<sup>15</sup> which is the maximum possible flux. Consequently, the conductance in Eq. (5) should also reach its maximum value. Note that this result might also be obtained from the expression of the Kapitza resistance by including a frequency independent transmission coefficient.

The model in Eq. (4) may be intentionally simple but it reveals the key mechanisms, i.e., the competition between the substrate resistance and the wire resistance. The comparison of our results to the predictions of phonon Green's functions, which are accepted as a rather fundamental and precise approach, is satisfactory because a mismatch of 10% is obtained. Also note that a recent work<sup>17</sup> showed that the elasticity based descriptions used in previous studies generate more than 10% error on the bending rigidity compared to *ab initio* predictions when applied to silicon beams of breadths smaller than 20 nm because of elastic surface effects. It reveals that the accuracy of the classical elastic model is in the same range as the one defined by the variations of the values predicted by several other models, i.e., acoustic mismatch, diffuse limit, and Green's functions.

The products  $C_{b,w} v_{b,w}$  are calculated from the temperature derivatives of the heat fluxes  $Q_{b,w}$ ,

$$\frac{\partial Q_{b,w}}{\partial T} = \frac{1}{V} \sum_m \sum_{\mathbf{k}>0} \hbar \omega_{m,\mathbf{k}} \frac{\partial \tilde{n}}{\partial T} v_{m,\mathbf{k}}, \quad (6)$$

where  $v_{m,\mathbf{k}} \cos \theta$  denotes the projection of the group velocity of the mode of frequency  $\omega_{m,\mathbf{k}}$  and wave vector  $\mathbf{k}$  in the wire

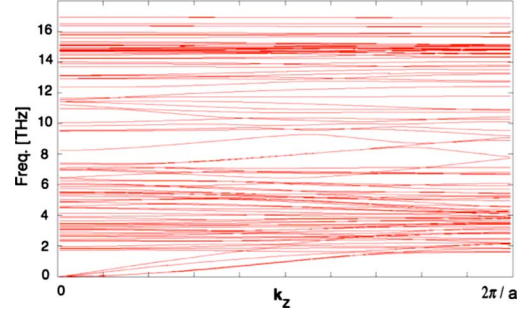


FIG. 1. (Color online) Dispersion curves in a silicon nanowire with a square cross section of  $2 \times 2$  cubic cells.  $a$  refers to the size of the cubic cell.

axis direction. The index  $m$  refers to the phonon branch and  $\tilde{n}$  is the Bose-Einstein distribution.  $V=L^3$  corresponds to the volume of the system. For the substrate, heat flux  $Q_b$  includes the contributions coming from directions of one-half space. Rewriting Eq. (6) for the thermal reservoir in more details yields

$$C_b v_b = \frac{\partial Q_b}{\partial T} = \pi \frac{g_{3D}}{V} \sum_m \int_0^{2\pi/a} \hbar \omega_{m,\mathbf{k}} \frac{\partial \tilde{n}}{\partial T} v_{m,\mathbf{k}} k^2 dk. \quad (7)$$

The isotropy of the group velocity  $v_{m,\mathbf{k}}$  is assumed and  $g_{3D} = \frac{V}{(2\pi)^3}$  is proportional to the phonon density of states of a three-dimensional lattice. The expression for  $C_w v_w$  follows Eq. (7) but the DOS corresponds to a 1D structure and  $g_{1D} = L/\pi$ . The integration over directions is removed and so is the velocity projection:

$$C_w v_w = \frac{\partial Q_w}{\partial T} = \frac{g_{1D}}{V} \sum_m \int_0^{2\pi/a} \hbar \omega_{m,\mathbf{k}} \frac{\partial \tilde{n}}{\partial T} v_{m,\mathbf{k}} dk. \quad (8)$$

### C. Nanowire-dispersion curves

Equations (7) and (8) can be fully calculated by determining group velocities and eigenfrequencies from phonon-dispersion curves. We hence compute them on the basis of classical lattice dynamics.<sup>18</sup> The Stillinger-Weber potential<sup>19,20</sup> used in those calculations provides the best overall description of the interatomic forces for the dispersion relations of semiconductor such as Si.

The dispersion relation for a nanowire having a cross section of  $2 \times 2$  cubic cells is plotted in Fig. 1. We check that phonon-dispersion curves include the bending and torsional modes that prove the validity of the boundary conditions.<sup>21,22</sup> When computing several wire diameters, we observe that the number of branches increases with cross section because it is proportional to the number of atoms per cell. The basic cell used to calculate the dispersion curves is a wire slice with a thickness equal to one lattice constant.

Group velocities are calculated as the derivation of the phonon branches with respect to wave vectors. In Fig. 2, the spectrum of group velocities shows that enlarging cross section leads to the reduction in the average group velocity except in the low-frequency range. As the lateral dimension of the wire is extended, new modes with diagonal wave vectors

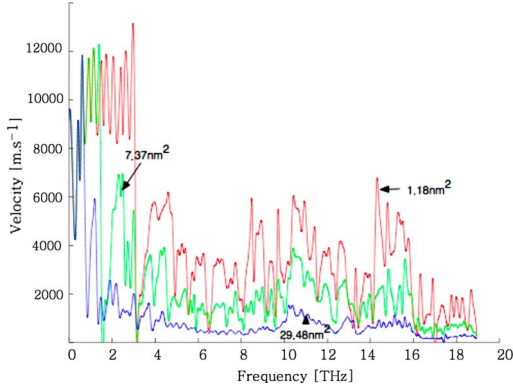


FIG. 2. (Color online) Branch averaged group velocity spectrum calculated for three wire cross sections.

appear. Those modes are stationary or with small group velocities because they undergo reflection on the free surfaces.

### III. RESULTS AND DISCUSSION

In Fig. 3, nanowires and contact thermal conductances are reported according to temperature for cross sections of 1.17, 7.37, 29.5, and 118.9 nm<sup>2</sup> corresponding to square edges of lengths  $d=1.08$ , 2.74, 5.43, and 10.9 nm, respectively. The intrinsic thermal conductance of the wire was estimated either by simply computing the term  $C_w v_w$ , which is the ballistic heat flux in the wire, or by using the quantum of conductance.<sup>12</sup> In this last approach, the four branches in the low-temperature regime were considered in the low-temperature regime. Note that additional terms accounting for higher-temperature contributions would increase the discrepancy between contact and wire conductances. However, the most striking point in Fig. 3 is that the contact conductance is smaller than the wire resistance—whatever the wire radius and the calculation method—by 2–3 orders of magnitude below 10 K. From Eq. (5), we deduce that this drastic deviation is due to the following condition:  $C_b v_b \ll C_w v_w$ . This implies that the contact conductance equals  $C_b v_b$  and becomes independent from the wire cross section. We have previously shown that the branch averaged group velocity  $v_w$  is smaller than the one in the reservoir. It follows that the physical explanation for the small contact conductance is the decrease with temperature of the heat capacity in the reservoir. This is the well-known  $T^3$  dependence of heat capacity in conventional three-dimensional crystals. This  $T^3$  law is hence retrieved at low temperatures for the thermal conductance at contact in Fig. 3.

We emphasize here that the observed resistance is due to the decrease in excited modes in the substrate, which appears through the decrease in heat capacity. This result appears as a clear justification to previous works<sup>9,10</sup> where a  $T^3$  dependence was found for the conductance including wire and contacts.

From these physical considerations, we also predict the temperature dependences of wire-membrane and membrane-plane substrate conductances. The membrane being considered as a two-dimensional system, a  $T^2$  evolution of the conductance is expected in the first case. In the latter case of the

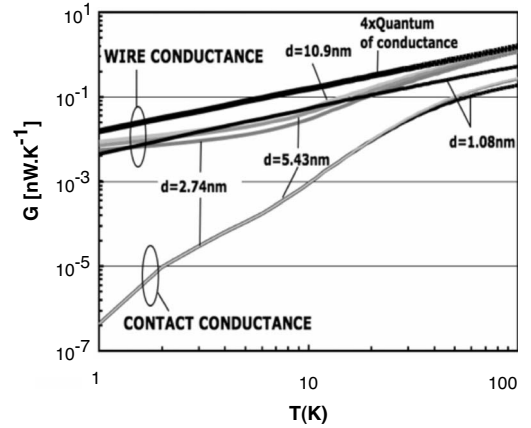


FIG. 3. Thermal conductance of contact between wires and substrate compared to conductances of the wires—calculated from  $C_w v_w$  and the quantum of conductance (Ref. 12)—versus temperature. The quantity  $d$  refers to the size of the edge of the squared cross section. The conductance in  $\text{W m}^{-2} \text{K}^{-1}$  of Eq. (3) was rescaled by the wires' cross sections.

membrane-plane substrate contact, a  $T^3$  law related to the planar substrate behavior is again expected. The quantitative results for those conductances are obtained from the calculation of the term  $C_b v_b$  applied to the substrate being either a membrane or the plane substrate.

We also deduce that the extension of the temperature gradient inside the substrates becomes extremely large because phonons entering the substrate have very few collisions with the ones of the substrate. This is a point that should be considered when carrying out experiments with micron scale heaters.

The DOS in the wire is a constant and its heat capacity is hence proportional to temperature. Figure 3 clearly confirms this dependence for the prediction based on the quantum of conductance and for the wire with smallest cross section. Wires with larger cross sections might not exhibit the rigorous behavior of a 1D structure, which might explain the slight deviation from the  $T^1$  law. We also note that the conductance remains smaller than 0.001 nW/K below 10 K,<sup>23</sup> whereas the phonon-particle approach predicts a value larger than 1 nW/K.<sup>24</sup> This corroborates the predominance of the wave effect on the contact conductance.

We also report on the influence of the crystalline orientations [100] and [111] of the Si wire. Results show that discrepancies between both orientations are only observed at very low temperatures. From 100 to 5 K, the discrepancy increases from 10% to 60% for any wire cross section, as shown in Fig. 4. At room temperature, the gap between the contact conductances derived from both crystalline orientations can be neglected.

To sum up, thermal conductances due to the contact are clearly 1–3 orders of magnitude smaller than wires conductances below 10 K. This result implies that heat transfer in a long wire with a sub-10-nm diameter is driven by the contacts. We therefore believe that measurements of the quantum of conductance in nanowires are not feasible when heating is introduced through connections. This statement is restricted to temperature domains where the predominant

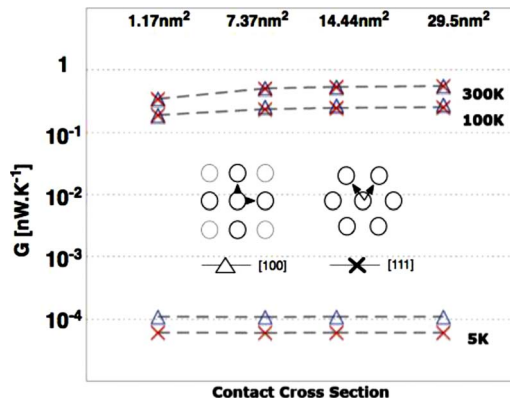


FIG. 4. (Color online) Comparison of thermal conductance for different lattice orientation defining the contact shape.

phonon wavelength is on the same order of magnitude or smaller than the wire diameter. Conductance data might exhibit a  $T^{2-3}$  dependence at low temperatures but our demonstration shows that it might well be an artifact related to the properties of the substrate. Nanotubes have dimensions varying between 2 and 3; they are therefore not targeted by our conclusions.

#### IV. CONCLUSION

The studied wires have square cross sections with edges ranging from 1 to 10 nm in such a way that phonon wave effects are predominant. The thermal conductance at contact was estimated by using the approximate model of the diffuse limit for the transmission coefficient at wire/substrate interface. However this model provides a large conductance for the contact, which ensures the robustness of our conclusions. Also note that previous works<sup>16</sup> showed that the discrepancy between the predictions of the diffuse limit model and of more sophisticated descriptions remain smaller than about 10%. In this range, the presented results still have a quantitative relevance.

We have shown that the conductance at contact is 2–3 orders of magnitude smaller than the conductance of the wire

below 10 K. Any changes in the contact shape, in the estimation of the wire contribution, or in the transmission model would increase the gap between the two conductances. We hence claim that heat conduction in nanowires with sub-10-nm diameters is driven by the conductance at contact and more precisely by the substrate contribution. The basic reason for the discrepancy between both conductance is a mismatch in phonon DOS. The contact conductance exhibits a  $T^3$  dependence at very low temperatures  $T < 30$  K, which proves that the substrate produces the predominant resistance for the wire. From these physical considerations, we have also deduced the temperature dependences of wire-membrane and membrane-plane substrate conductances. The membrane being considered as a two-dimensional system, a  $T^2$  evolution of the conductance is expected in the first case. In the latter case of the membrane-plane substrate contact, a  $T^3$  law related to the planar substrate behavior is again expected.

Showing the major role of contact conductance might explain the difficult interpretation of the measurements of nanowire thermal conductances. It also emphasizes the major role of the contact shape when designing nanocircuits and nanoprobe. We expect the damaging threshold to be much quickly reached and the burn out to be observed in the contact zone. The analysis can be extended by performing molecular-dynamics simulations to have a more accurate description of the transmission mechanisms. However, comparison between our results and those obtained from Green's-function approach<sup>21,22</sup> already tends to be satisfactory.

#### ACKNOWLEDGMENTS

We thank N. Mingo and K. Joulain for useful discussions. We also thank D. Gale for having released the General Utility Lattice Program (GULP) under free license. The financial support of the National Agency for Research (program ANR/PNANO 2006, project NANOTHERMOFLUO under Grant No. ANR-06-NANO-004) is gratefully acknowledged.

\*yann.chalopin@em2c.ecp.fr

<sup>1</sup>Y. Cui and M. Lieber, *Science* **291**, 851 (2001).

<sup>2</sup>M. W. Shao, Y.-Y. Shan, N.-B. Wong, and S.-T. Lee, *Adv. Funct. Mater.* **15**, 1478 (2005).

<sup>3</sup>Y. T. Yang, C. Callegari, X. L. Feng, K. L. Ekinci, and M. L. Roukes, *Nano Lett.* **6**, 583 (2006).

<sup>4</sup>S. Volz and G. Chen, *Appl. Phys. Lett.* **75**, 2056 (1999).

<sup>5</sup>S. Volz and D. Lemonnier, *Phys. Low-Dimens. Semicond. Struct.* **5/6**, 91 (2000).

<sup>6</sup>S. Volz, D. Lemonnier, and J.-B. Saulnier, *Microscale Thermophys. Eng.* **5**, 191 (2001).

<sup>7</sup>R. Prasher, T. Tong, and A. Majumdar, *Nano Lett.* **8**, 99 (2008).

<sup>8</sup>K. Schwab, E. A. Henriksen, J. M. Worlock, and M. L. Roukes, *Nature (London)* **404**, 974 (2000).

<sup>9</sup>C. Dames and G. Shen, *J. Appl. Phys.* **95**, 682 (2004).

<sup>10</sup>C. M. Chang and M. R. Geller, *Phys. Rev. B* **71**, 125304 (2005).

<sup>11</sup>R. Prasher, *J. Appl. Phys.* **102**, 104312 (2007).

<sup>12</sup>L. G. C. Rego and G. Kirczenow, *Phys. Rev. Lett.* **81**, 232 (1998).

<sup>13</sup>J. Zou and A. Balandin, *J. Appl. Phys.* **89**, 2932 (2001).

<sup>14</sup>M. C. Cross and R. Lifshitz, *Phys. Rev. B* **64**, 085324 (2001).

<sup>15</sup>G. Chen, *J. Heat Transfer* **118**, 539 (1996).

<sup>16</sup>G. Chen, *Phys. Rev. B* **57**, 14958 (1998).

<sup>17</sup>R. Maranganti and P. Sharma, *Phys. Rev. Lett.* **98**, 195504 (2007).

<sup>18</sup>N. Mingo, *Phys. Rev. B* **68**, 113308 (2003).

<sup>19</sup>F. H. Stillinger and T. A. Weber, *Phys. Rev. B* **31**, 5262 (1985).

<sup>20</sup>Zi Jian, Zhang Kaiming, and Xie Xide, *Phys. Rev. B* **41**, 12915 (1990).

<sup>21</sup>N. Mingo and L. Yang, *Phys. Rev. B* **68**, 245406 (2003).

<sup>22</sup>N. Mingo, *Phys. Rev. B* **74**, 125402 (2006).

<sup>23</sup>R. Prasher, *Nano Lett.* **5**, 2155 (2005).

<sup>24</sup>S. Volz and P.-O. Chapuis, *J. Appl. Phys.* **103**, 034306 (2008).